INTERNATIONAL SOCIETY FOR
SOIL MECHANICS AND
GEOTECHNICAL ENGINEERING

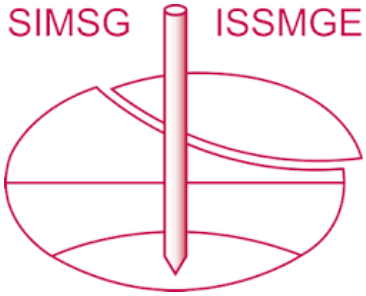

This paper was downloaded from the Online Library of the International Society for Soil Mechanics and Geotechnical Engineering (ISSMGE). The library is available here:

https://www.issmge.org/publications/online-library

This is an open-access database that archives thousands of papers published under the Auspices of the ISSMGE and maintained by the Innovation and Development Committee of ISSMGE.

Geotechnical Aspects of Underground Construction in Soft Ground – Viggiani (ed)
© 2012 Taylor & Francis Group, London, ISBN 978-0-415-68367-8

Bearing capacity analysis of cohesive-frictional soils with dual circular tunnels

K. Yamamoto
Department of Ocean Civil Engineering, Kagoshima University, Kagoshima, Japan

A.V. Lyamin, D.W. Wilson, A.J. Abbo & S.W. Sloan
Centre for Geotechnical and Materials Modelling, University of Newcastle, NSW, Australia

ABSTRACT: The ultimate bearing capacity and the failure mechanism of cohesive-frictional soils with the inclusion of dual circular tunnels have been theoretically and numerically investigated assuming plane strain conditions. Unlike the case of a single tunnel, the center-to-center distance appears as a new problem parameter, which plays a key role in tunnel stability. A continuous loading is applied to the ground surface. For a series of tunnel diameter to depth ratios and material properties, rigorous lower and upper bound solutions for the ultimate bearing capacity of the considered soil mass are obtained by applying recently developed numerical limit analysis. For practical suitability the results are presented in the form of dimensionless stability charts. As an additional check and also a handy practical means, upper bound rigid block mechanisms for dual circular tunnels have been developed and the predicted collapse loads compared with the results from numerical limit analysis.

1 INTRODUCTION

The accurate assessment of the stability of foundations above shallow tunnels is a very important task due to the increasing demand on construction of buildings and tunnels in urban areas. Unfortunately, no generally accepted design or analysis method is available at the moment to evaluate the ultimate bearing capacity of cohesive-frictional soils with shallow tunnel inclusions. The design of tunnels for roads and railways often utilize separate tunnels to carry traffic in opposite directions. Also, in the expansion of underground transportation systems new tunnels have recently been designed and then constructed near existing tunnels. In practice, it is often seen that the construction of dual circular tunnels is a better option than a single large circular tunnel.

In this paper, the ultimate bearing capacity and failure mechanisms of cohesive-frictional soils with dual circular tunnels have been theoretically and numerically investigated assuming plane strain conditions. Compared to the case of a single circular tunnel, the effect of center-to-center distance on dual circular tunnels is naturally a key factor. In addition, it is assumed that the problem of interaction between dual tunnels is more complex due to the geometry of the tunnels and the properties of the lining and surrounding soils. Drained loading conditions are considered, the internal tunnel pressure is set to zero, and a continuous load is applied to the ground surface. Both smooth and rough interface conditions between the loading and soil are modelled. For a series of tunnel diameter to depth ratios and material properties, rigorous lower and upper bound solutions for the ultimate bearing capacity of the considered soil mass are obtained by applying recently developed numerical limit analysis techniques (Lyamin & Sloan 2002, Krabbenhøft *et al*. 2005). For practical suitability the results are presented in the form of dimensionless stability charts, with the actual bearing capacities being closely bracketed from above and below. As a validation of the results and also as a convenient practical calculation, upper bound rigid block mechanisms for dual circular tunnels have been developed and the obtained values of collapse loads are compared with the results of the numerical limit analysis.

The application of computational limit analysis to the stability of shallow tunnels has been pioneered by Sloan & Assadi (1992) who investigated the stability of a plane strain tunnel in a cohesive soil with shear strength varying linearly with depth using linear programming techniques. The stability of the tunnel was described conveniently by two load parameters $(\sigma_s - \sigma_t)/c_{u0}$ and $\gamma D/c_{u0}$. Lyamin & Sloan (2000) considered the stability of a plane strain circular tunnel in a cohesive-frictional soil. The nonlinear programming technique

was applied which allowed a vast shortening of the computational time as well as increasing the number of finite elements, thus resulting in very accurate solutions. The drained stability of the tunnel was described by the load parameters σ_t / c'. In addition, Wilson *et al*. (2008) investigated the undrained stability of dual square tunnels using numerical limit analysis and rigid block upper bound methods. Stability charts were generated for a variety of tunnel depths, material properties and inter-shaft distances. Recently, Yamamoto *et al*. (2009) initiated investigation of the ultimate bearing capacity and the failure mechanism of cohesive-frictional soils with a shallow circular tunnel. The upper bound rigid block mechanisms were also developed and the computed collapse loads compared with the results of numerical limit analysis. This paper presents the extension of this research to dual circular tunnels.

2 PROBLEM DESCRIPTION

The dual circular tunnel problem to be considered is presented in Figure 1. The ground is modelled as a uniform Mohr-Coulomb material with a cohesion c', friction angle ϕ' and unit weight γ, assuming drained loading conditions. The tunnel is of diameter D, depth H and the center-to-center distance S, and the internal tunnel pressure is set to zero ($\sigma_t = 0$). The ultimate bearing capacity of cohesive-frictional soils with the inclusion of dual circular tunnels is described conveniently by the dimensionless load parameter σ_s / c' which is a function of ϕ', $\gamma D / c'$, H/D, S/D and L/D, as shown in Eq. (1).

$$\sigma_s / c' = f(\phi', \gamma D / c', H / D, S / D, L / D) \tag{1}$$

As continuous loading is applied to the ground surface the L/D parameter may be eliminated from equation (1). Formulating the problem in this manner permits a compact set of stability charts to be constructed using the 4 remaining dimensionless parameters. The range of parameters considered in this paper are $H/D = 1$–5, $\phi' = 0^\circ$–20, $\gamma D / c' = 0$–3 and tunnel spacing $S/D = 0$–11. Both smooth and rough interface conditions between the loading and soil are considered.

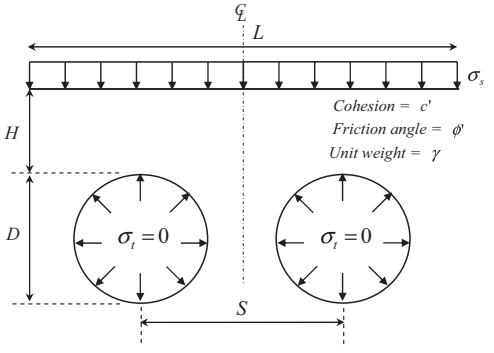

Figure 1. Plane strain dual circular tunnels in cohesive-frictional soil.

3 NUMERICAL LIMIT ANALYSIS

Limit analysis utilizes the power of lower and upper bound theorems of plasticity theory to provide rigorous bounds on collapse loads from both below and above. The theorems themselves are based on the principle of maximum power dissipation, which is valid for soil following an associated flow rule. The use of finite element discretization of the soil combined with mathematical optimization to maximize lower bound and minimize upper bound has now made it possible to handle routine problems with complex geometries and loading conditions. The formulations of numerical limit analysis used in this paper originate from those given by Sloan (1988, 1989) and Sloan & Kleeman (1995) who employed active set linear programming and discontinuous stress and velocity fields to solve variety of stability problems. Since then, numerical limit analysis has evolved significantly and the techniques used in this paper are those described in Lyamin & Sloan (2002) and Krabbenhøft *et al*. (2005).

Figure 2 show the lower bound and upper bound half-mesh for H/D = 1 and S/D = 2 with smooth interfaces. The mesh is symmetric, and

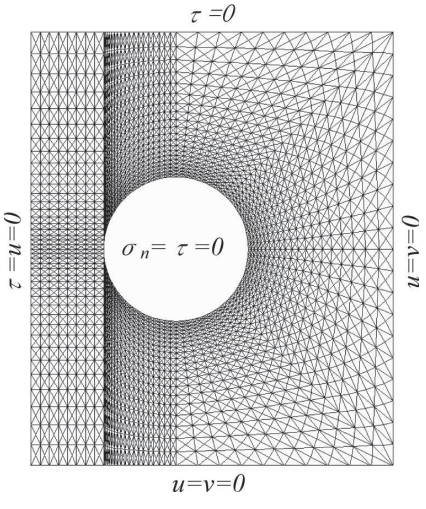

Figure 2. Finite element mesh for H/D = 1 and S/D = 2 showing boundary conditions for numerical limit analysis.

similar meshes are used for lower and upper bound analyses. Typical lower/upper bound mesh has 7680 triangular elements and 11412 stress/velocity discontinuities. In the lower bound analysis, extension elements are included along the soil domain boundaries to represent a semi-infinite material. When the width of loading, L, equals $2H + D + S$ in Fig. 2, the loading is regarded as the infinite width loading, because the whole failure mechanism is included within the domain. Careful mesh refinement around the tunnel is required to get accurate solutions. The mesh is particularly dense around the tunnel and is smoothly connected from the tunnel face toward the boundary.

4 UPPER BOUND RIGID BLOCK ANALYSIS

Semi-analytical rigid block methods were used in this study to find the upper bound solutions for the problems considered. These solutions provide an additional check on the finite element limit analysis results and will be able to also serve as simple design tools for practicing engineers. Three types of rigid block mechanisms were constructed as shown in Figure 3. In this Figure, A_i is the area of the rigid block; V_i is the kinematically admissible velocity of block i; V_{ij} is the velocity jump along the discontinuity between blocks i and j; l_{ij} is the length of the discontinuity between blocks i and j; α, β, γ, δ, ε, λ and ω are the angular parameters which determine the geometry of the rigid block mechanisms for mechanism 1 (θ is dependent parameter for mechanism 1); ϕ' is the dilatancy angle. Mechanism 1 is a simple roof and side collapse mechanism typically suitable for shallow tunnels, while mechanisms 2 and 3 are more complex and are characterized by collapse of both the roof and side of the tunnel. The total numbers of unknown angular parameters in each of the mechanisms are 7, 8 and 12 respectively. The behavior of the soil mass was assumed to be governed by Mohr-Coulomb failure criterion and an associated flow rule. The geometry of the blocks is allowed to vary while being constrained such that their areas and boundary segments lengths stay positive. The details of rigid block analysis can be found in Chen (1975).

The minimum upper bound solution for each mechanism was obtained by optimizing its geometry using the Hooke & Jeeves algorithm with discrete steps (Bunday, 1984). This method works by performing two different types of searches, an exploratory search and a pattern search. The rigid block analyses are extremely quick taking of the order of just one second. Provided an appropriate mechanism is chosen, this technique gives a fairly accurate upper bound estimate which can be used

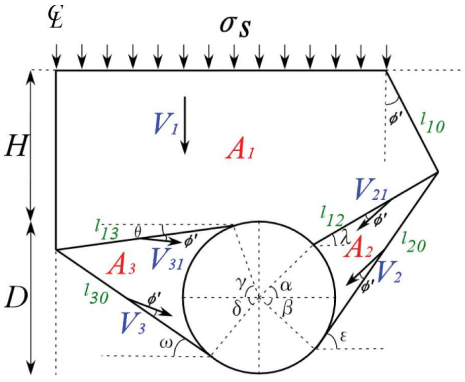

(a) mechanism 1

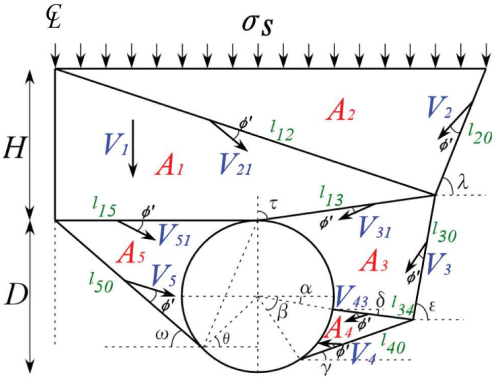

(b) mechanism 2

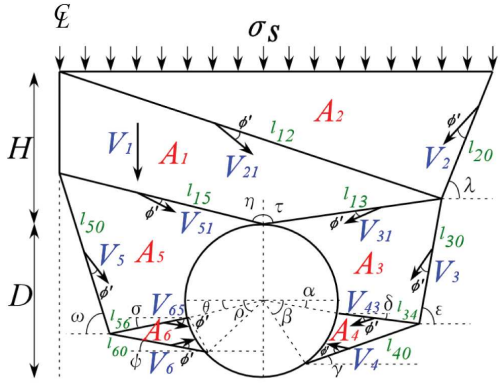

(c) mechanism 3

Figure 3. Upper bound rigid block mechanisms for dual circular tunnels.

to check the finite element solutions and does not require significant computational efforts.

5 RESULTS AND DISCUSSION

Figures 4–6 show the plastic zones (a), power dissipations (b) and rigid block mechanisms (c) for the dual circular tunnels. The plastic zones and power dissipations are obtained from the numerical lower and upper bound limit analyses and the rigid block mechanism is obtained from the upper bound rigid block analysis. The intensity of plastic zones and power dissipations are shown by the color shading. The dimensionless load parameter σ_s / c' of the lower and upper bound solutions obtained from the numerical limit and rigid block analyses is included in each figure. It is found from Figures 4a and 4b that for tunnels of a relatively shallow depth, small that for tunnels of a relatively shallow depth, small friction angles and close center-to-center spacing, a small slip surface originates between dual circular tunnels and a large slip surface originates at top on the outside of the tunnels. The large slip surface curves toward the ground surface. As can be seen from these figures the failure mechanisms of the rigid block technique agree well with those observed in the plastic zones and power dissipations. For the case of moderate depth, small friction angles and close center-to-center spacing presented in Figures 5a and 5b, a small slip surface between dual circular tunnels enlarges to cover the top and bottom of the tunnel and the large slip surface originates around the outer side of the pair of tunnels. The ultimate bearing capacity in this case is higher than that shown in Figure 4 due to increase of H/D and S/D. The upper bound solutions (Figs. 4–5c) obtained from the rigid block technique are in good agreement with those from the numerical limit analysis (Figs. 4–5b). Figure 6 shows the case of deep depth, small friction angles and moderate center-to-center distance. The slip surface between dual circular tunnels enlarges to encompass the entire tunnel and the large slip surface originates around the bottom of the tunnel. It is observed from Figures 6a and 6b that the plastic zones have developed around the entire tunnel. In this case, the rigid block results (Fig. 6c) tend to be larger than the results of numerical limit analysis (Fig. 6b) due to the deep depth and moderate center-to-center distance.

When H/D and S/D increase, as shown in Figures 4–6, the failure mechanism slowly extends vertically and transversely to eventually encompass the entire tunnel. These deeper and wider collapse mechanisms are more complex than those for shallow and narrow ones. The rigorous lower and upper bound solutions bracket the true ultimate bearing capacity quite accurately for the case of small frictional angles. It is found from Figures 4–6 that the S/D parameter has a key role for the pattern of failure mechanism and the increase of bearing capacity due to the effect of interaction. Of the several developed rigid block mechanisms shown in Figure 3, the best upper bound solutions were almost always obtained from mechanisms 1 and 3, which consist of three and six rigid blocks. In general, mechanism 1 is suitable for the cases of shallow tunnels with low friction angles and mechanism 3 for the case of deeper tunnels and high friction angles. In the case of moderate ϕ' and H/D, when S/D is increased, the best upper bound solutions started to be produced from mechanism 3. For the case of $\phi' = 20^\circ$, all the best upper bound solutions were obtained from mechanism 3. Additionally, the upper bound solutions obtained from the rigid block and numerical limit analyses are in good agreement (Figs. 4–5b, c), with the rigid block results tending to be larger than the limit analysis ones when H/D or ϕ' or S/D increases. This is due to the assumption that failure mechanism extends from the ground surface into the soil mass with the inclination angle equal to the friction angle ϕ'. Also, tunnels with a deeper and wider center-to-center configuration have a more complex collapse pattern, therefore, the simple rigid block mechanisms proposed in this study are generally less accurate for deeper and moderate distance tunnels than for shallow and close distance ones. Furthermore, it is more difficult to propose an efficient rigid block mechanism in the case of cohesive-frictional soils than in the case of purely cohesive material. As shown in Figure 6, the collapse mechanism for deeper and moderate distance tunnels is quite wide at the surface as well as it extends further around the bottom of the tunnel. Even using mechanism 3, the feasible solutions could not be easily obtained for high values of H/D or ϕ' or S/D.

Figures 7–8 shows the comparison of stability numbers obtained from both numerical limit and rigid block analyses. The interface condition is smooth. The lower and upper bound solutions of the numerical limit analysis for each $\gamma D / c'$ are plotted using broken and solid lines, respectively. As a general trend for all considered cases it can be observed from Figures 7 and 8 that stability numbers decrease when $\gamma D / c'$ increases. It is found that the ultimate bearing capacity increases monotonically with the increase of S/D, except for the cases of close proximity, $S/D \le 2.0$ (Fig. 8a) and $S/D \le 3.0$ (Fig. 8b). For the cases of 1) $H/D = 1$ and $\phi' = 10^\circ$, $S/D \le 3.0$, 2) $H/D = 1$ and $\phi' = 20^\circ$, $S/D \le 2.0$, 3) $H/D = 3$ and $\phi' = 10^\circ$, $S/D \le 4.0$ and 4) $H/D = 4$ and $\phi' = 10^\circ$, $S/D \le 3.5$, it is found that the upper bound solutions from the rigid block method have relatively good agreement with those

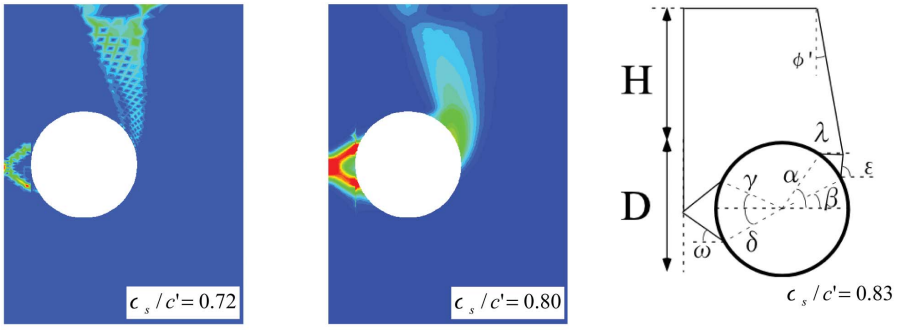

(a) plastic zones (b) power dissipation (c) rigid block mechanism

Figure 4. Comparison of numerical limit analysis with rigid block mechanism ($H/D = 1$, $\phi' = 10°$, $\gamma D/c' = 1$, $S/D = 1.5$, smooth interface).

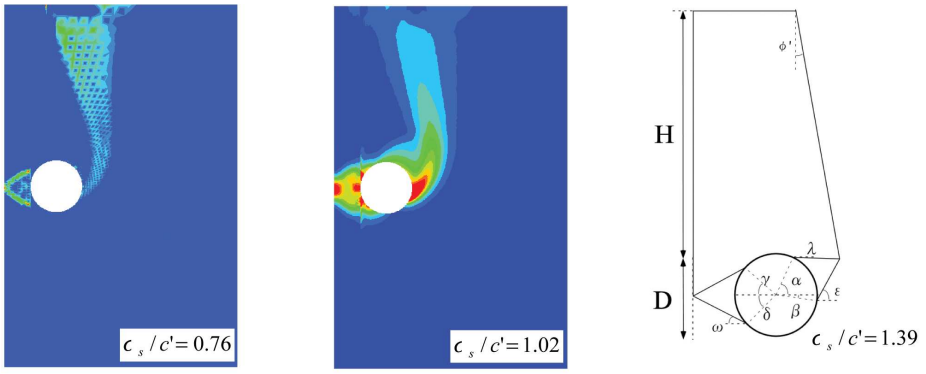

(a) plastic zones (b) power dissipation (c) rigid block mechanism

Figure 5. Comparison of numerical limit analysis with rigid block mechanism ($H/D = 3$, $\phi' = 10°$, $\gamma D/c' = 1$, $S/D = 2.0$, smooth interface).

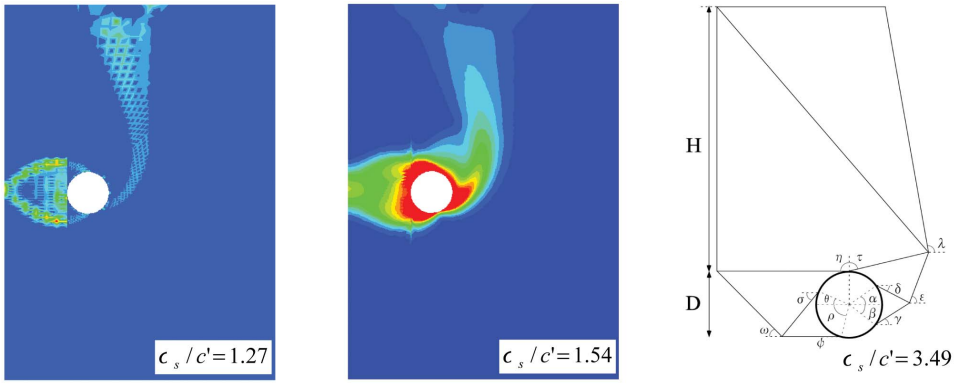

(a) plastic zones (b) power dissipation (c) rigid block mechanism

Figure 6. Comparison of numerical limit analysis with rigid block mechanism ($H/D = 4$, $\phi' = 10°$, $\gamma D/c' = 1$, $S/D = 4.0$, smooth interface).

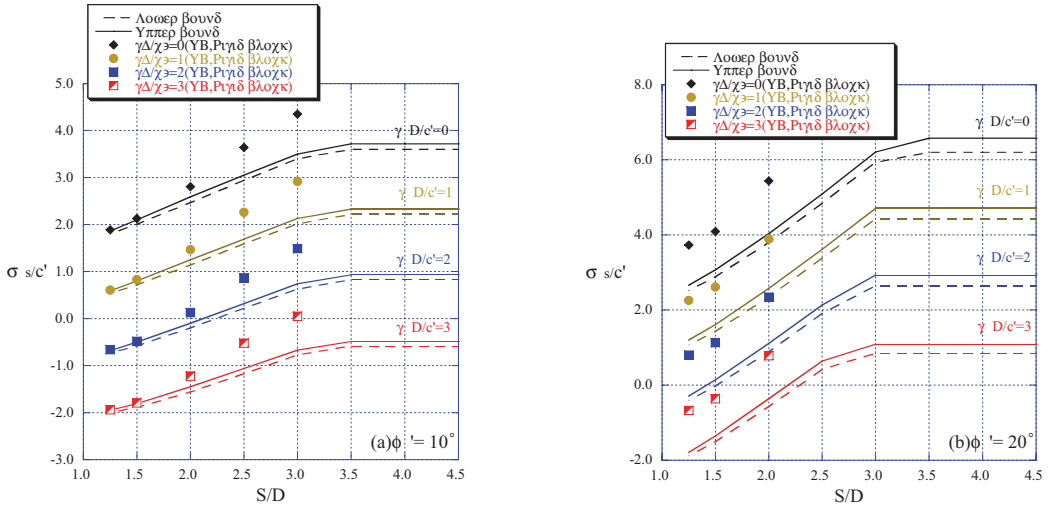

Figure 7. Stability bounds for dual circular tunnels (H/D=1, ϕ' = 10°, 20°, smooth interface).

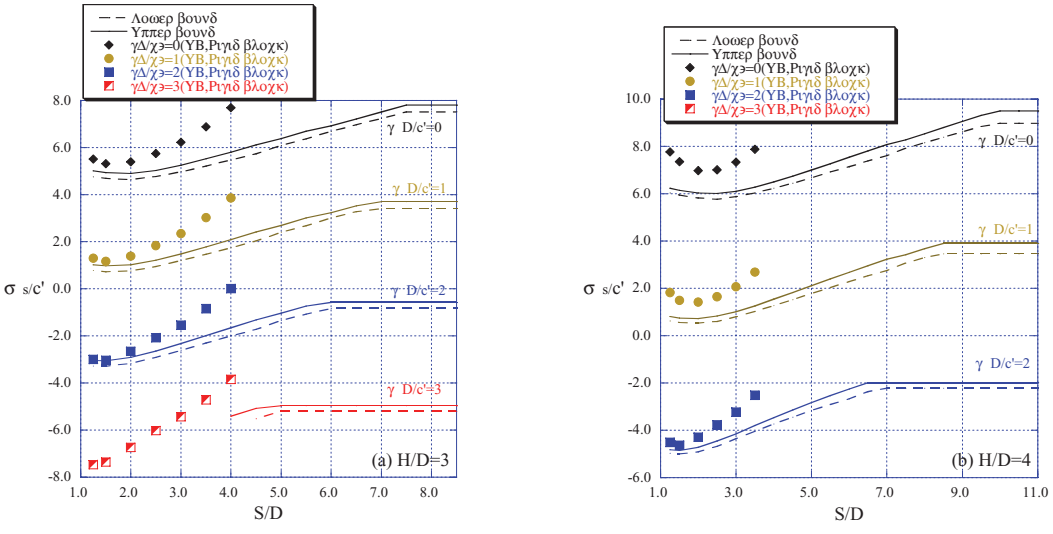

Figure 8. Stability bounds for dual circular tunnels (H/D =3,4, ϕ' = 10°, smooth interface).

obtained from the numerical limit analysis. But, with the increase of S/D the accuracy of considered rigid block mechanisms becomes poor. In most cases of $\gamma D / c' = 3$, $S / D \le 4.5$ (Fig. 8a) and $\gamma D / c' = 3$ (Fig. 8b), the feasible solutions from the rigid block and numerical limit analyses could not be obtained because the tunnel collapses under soil self weight. It is important to mention the sign convention used for stability numbers presentation. A positive value of stability number implies that a compressive normal stress can be applied to the ground surface up to this value, while a negative stability number means that we can only apply a tensile normal stress to the soil surface (no bearing capacity in normal sense). The negative range of stability numbers is likely to be of less practical interest than the positive ones. When S/D increases further, the lower and upper bound solutions of the numerical limit analysis tend to become constant at certain point, e.g. at $S / D = 3.5$ for $\gamma D / c' = 0 - 3$ (Fig.7a). The plots of plastic zones and power dissipations show no interaction between dual

circular tunnels at such points and after that the failure mechanism becomes that of two individual single tunnels failing independently. Thus, these points are regarded as the no interaction points for dual circular tunnels and this information would be important for engineering practice. Also, it is found that the no interaction points decreases when $\gamma D / c'$ increases for each H/D and ϕ'.

6 CONCLUSIONS

The ultimate bearing capacity and the failure mechanisms of cohesive-frictional soils with the inclusion of dual circular tunnels have been investigated and rigorous bounds on the stability numbers computed assuming plane strain conditions. The results of these analyses have been presented in the form of dimensionless stability charts. As an additional check of the validity of the numerical limit analysis several rigid block mechanisms for dual circular tunnels have been developed. Comparison of upper bound solutions obtained from the rigid block analysis with those of the numerical limit analysis shows good agreement when H/D, ϕ' and S/D are small.

For the cases in which the dual tunnels are deeper and in close proximity, it has been confirmed that the bearing capacity exhibits a slight decrease due to the interaction between pair of circular tunnels. Also, the interaction tends to disappear when the center-to-center distance exceeds a certain value (no interaction point). For future work, it is proposed to develop suitable for practical use rigid block mechanisms which are efficient also for high frictional angles and moderate center-to-center distance.

REFERENCES

Bunday, B.D. 1984. Basic optimisation methods. Edward Arnold.

Chen, W.F. 1975. Limit analysis and soil plasticity. Elsevier, Amsterdam.

Krabbenhøft, K., Lyamin, A.V., Hjiaj, M. & Sloan, S.W. 2005. A new discontinuous upper bound limit analysis formulation. *International Journal for Numerical Methods in Engineering*, 63: 1069–1088.

Lyamin, A.V. & Sloan, S.W. 2000. Stability of a plane strain circular tunnel in a cohesive-frictional soil. In D.W. Smith & J.P. Carter (eds), *Developments in theoretical geomechanics*, Balkema, Rotterdam, 139–153.

Lyamin, A.V. & Sloan, S.W. 2002. Lower bound limit analysis using non-linear programming. *Int. J. Numer. Meth. Engng.*, 55: 573–611.

Sloan, S.W. 1988. Lower bound limit analysis using finite elements and linear programming. *Int. J. Numer. Analyt. Meth. Geomech.*, 12: 61–77.

Sloan, S.W. 1989. Upper bound limit analysis using finite elements and linear programming. *Int. J. Numer. Analyt. Meth. Geomech.*, 13: 263–282.

Sloan, S.W. & Assadi, A. 1992. Stability of shallow tunnels in soft ground. In G.T. Houlsby & A.N. Schofield (eds), *Predictive soil mechanics*, Thomas Telford, London, 644–663.

Sloan, S.W. & Kleeman, P.W. 1995. Upper bound limit analysis using discontinuous velocity fields. *Comp. Methods in Appl. Mech. and Engng.*, 127: 293–314.

Wilson, D.W., Abbo, A.J., Sloan, S.W. & Lyamin, A.V. 2008. Undrained stability of dual square tunnels. In D.N. Singh (ed.), *Proc. of the 12th Int. Conf. of Int. Assoc. for Comp. Methods and Advances in Geomechanics (IACMAG)*, Goa, India.

Yamamoto, K., Lyamin, A.V., Wilson, D.W., Abbo, A.J. & Sloan, S.W. 2009. Limit analysis of shallow tunnels in cohesive frictional soils. In G. Meschke, G. Beer, J. Eberhardsteiner, D. Hartmann & M. Thewes (eds), *Proc. of 2nd Int. Conf. on Comp. Methods in Tunnelling*; *EURO:TUN 2009*, Bochum, 817–824.